

1N-37

7284

P33

NASA  
Technical Memorandum 103695

AVSCOM  
Technical Report 90-C-022

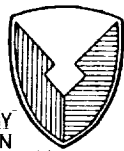
# Effects of Gear Box Vibration and Mass Imbalance on the Dynamics of Multi-Stage Gear Transmissions

Fred K. Choy and Yu K. Tu  
*The University of Akron*  
*Akron, Ohio*

and

James J. Zakrajsek and Dennis P. Townsend  
*Lewis Research Center*  
*Cleveland, Ohio*

March 1991



US ARMY  
AVIATION  
SYSTEMS COMMAND  
AVIATION R&T ACTIVITY

(NASA-TM-103695) EFFECTS OF GEAR BOX  
VIBRATION AND MASS IMBALANCE ON THE DYNAMICS  
OF MULTI-STAGE GEAR TRANSMISSIONS (NASA)  
33 p CSCL 13I

N91-21534

Unclass  
0007284

63/37



EFFECTS OF GEAR BOX VIBRATION AND MASS-IMBALANCE ON THE  
DYNAMICS OF MULTISTAGE GEAR TRANSMISSIONS

Fred K. Choy and Yu K. Tu  
Department of Mechanical Engineering  
The University of Akron  
Akron, Ohio 44325

James J. Zakrajsek and Dennis P. Townsend  
National Aeronautics and Space Administration  
Lewis Research Center  
Cleveland, Ohio 44135

ABSTRACT

The objective of this paper is to present a comprehensive approach to analyzing the dynamic behavior of multistage gear transmission systems, with the effects of gear-box-induced vibrations and rotor mass-imbances. The model method, using undamped frequencies and planar mode shapes, is used to reduce the degree-of-freedom of the system. The various rotor-bearing stages as well as the lateral and torsional vibrations of each individual stage are coupled through localized gear-mesh-tooth interactions. Gear-box vibrations are coupled to the gear stage dynamics through bearing support forces. Transient and steady state dynamics of lateral and torsional vibrations of the geared system are examined in both time and frequency domains. Vibration signature analysis techniques will be developed in interpret the overall system dynamics and individual modal excitations under various operating conditions. A typical three-staged geared system is used as an example. Effects of mass-imbalance and gear box vibrations on the system dynamic behavior are presented in terms of modal excitation functions for both lateral and torsional vibrations. Operational characteristics and conclusions are drawn from the results presented.

## NOMENCLATURE

$A_i(t)$	modal function of the $i^{\text{th}}$ mode in x-direction
$A_{ti}(t)$	modal function of the $i^{\text{th}}$ mode in $\theta$ -direction
$B_i(t)$	modal function of the $i^{\text{th}}$ mode in y-direction
$[C_T]$	torsional damping matrix
$[C_{xx}], [C_{xy}], [C_{yx}], [C_{yy}]$	bearing direct and cross-coupling damping matrices
$F_{Bx}, F_{By}$	bearing forces due to base motion
$F_{Gt}(t)$	gear mesh torque
$F_{Gx}(t), F_{Gy}(t)$	gear mesh force in x- and y-directions
$F_T(t)$	external excitation moment
$F_x(t), F_y(t)$	external excitation forces
$[G_A]$	gyroscopic-angular acceleration matrix
$[G_V]$	gyroscopic-angular rotation matrix
$[I]$	identity matrix
$[J]$	rotational mass moment of inertia matrix
$[K]$	average stiffness matrix
$K_s$	shaft stiffness matrix
$[K_T]$	torsional stiffness matrix
$K_{tik}$	gear mesh stiffness between $i^{\text{th}}$ and $k^{\text{th}}$ rotor
$K_{dx}, K_{dy}$	compensation matrices in x- and y-direction
$[K_{xx}], [K_{xy}], [K_{yx}], [K_{yy}]$	bearing direct and cross-coupling stiffness matrix
$[M]$	mass-inertia matrix
$R_{ci}$	radius of gear in the $i^{\text{th}}$ rotor
$X, Y$	generalized motion in x- and y-directions
$X_b, Y_b$	base motion in x- and y-directions

$X_{ci}, Y_{ci}$	gear displacements in x- and y-directions of the $i^{\text{th}}$ rotor
$\alpha_{ki}$	angle of tooth mesh between $k^{\text{th}}$ and $i^{\text{th}}$ rotor
$[\Lambda^2], [\Lambda_t^2]$	lateral and torsional eigenvalue diagonal matrices
$[\Phi]_k, [\Phi_t]_k$	lateral and torsional orthonormal eigenvector matrices of the $k^{\text{th}}$ rotor
$\phi_{kjl}$	$j^{\text{th}}$ orthonormal mode of $k^{\text{th}}$ stage at $l^{\text{th}}$ node

### INTRODUCTION

Presently there is a continuous search for the improvement in operational life, efficiency, maintainability, and reliability in gear transmission systems. With the increase in workload and speed requirements, the call for transmission design improvement becomes even greater. One of the major objectives in design improvement is the reduction of noise and vibration in the transmission system. Two main streams of work have been carried out in the areas of noise and vibration reduction; namely, (1) the localized gear tooth stress and thermal effects during gear interactions (Cornell 1981; Lin 1988; Boyd 1987; Savage 1986) and (2) the overall global dynamic behavior (August 1986; Choy 1989; David 1987, 1988; Mitchell 1985) of the transmission systems.

The work presented in this paper is the development and application of a comprehensive approach in simulating the overall dynamics of a multistage rotor-bearing-gear system. A system of rotor-bearing configurations with circular flexible shafts on flexible bearing supports are considered in this analysis. Excitations due to rotor mass-imbalance, shaft bow, and gyroscopic effects are considered in each individual rotor stage. Effects of base motion are incorporated through relative motion between rotor and casing at the

bearing supports. The dynamics of each rotor stage are coupled together at gear locations through nonlinear spring connections. The modal method is applied to reduce the degrees-of-freedom of the global system of equations into modal coordinates. The modal equations of motion are solved to evaluate system acceleration at each time step. A self-adaptive variable time-stepping integration technique (Choy 1987, 1988a, 1989) is used to calculate the transient dynamics of the system. A typical three-stage rotor-bearing-gear system is used as an example in this analysis. Results are presented in both time and frequency domains to develop vibration signature analysis of the system.

#### DEVELOPMENT OF EQUATIONS OF MOTION

The equations of motion for a single stage multimass rotor-bearing-gear system with the effects of gear-box-motion-induced vibrations at the bearing supports, rotor inertia-gyroscopic effects, and excitations from rotor mass-imbalance and residual runouts can be written in matrix form (Choy 1987, 1989) for the X-Z plane as

$$\begin{aligned}
 [M]\{\ddot{X}\} + [G_v]\{\dot{Y}\} + [C_{xx}]\{\dot{X} - \dot{X}_b\} + [C_{xy}]\{\dot{Y} - \dot{Y}_b\} + [G_A]\{Y\} \\
 + [K_{xx} + K_s]\{X\} - [K_{xx}]\{X_b\} + [K_{xy}]\{Y - Y_b\} = \{F_x(t)\} + \{F_{Gx}(t)\}
 \end{aligned} \tag{1}$$

and in the Y-Z plane as

$$\begin{aligned}
 [M]\{\ddot{Y}\} - [G_v]\{\dot{X}\} + [C_{yx}]\{\dot{X} - \dot{X}_b\} + [C_{yy}]\{\dot{Y} - \dot{Y}_b\} - [G_A]\{X\} \\
 + [K_{yy} + K_s]\{Y\} - [K_{yy}]\{Y_b\} + [K_{yx}]\{X - X_b\} = \{F_y(t)\} + \{F_{Gy}(t)\}
 \end{aligned} \tag{2}$$

Here  $F_x$  and  $F_y$  are force excitations from the effects of mass-imbalance and shaft residual bow in both x and y directions. Forces  $F_{Gx}$  and  $F_{Gy}$  are

the X and Y gear mesh forces induced from the gear teeth interaction with other coupled gear stages. The bearing forces are evaluated through the relative motion between the rotor {X}, {Y} and the gear box {X<sub>b</sub>}, {Y<sub>b</sub>} at the bearing locations (Choy 1987). The mass-inertia and gyroscopic effects are incorporated in the mass matrix [M] and the gyroscopic matrices [G<sub>v</sub>] and [G<sub>A</sub>]. The coupled torsional equations of motion for the single rotor-bearing-gear system can be written as

$$[J]\{\theta\} + [C_T]\{\dot{\theta}\} + [K_T]\{\theta\} = \{F_T(t)\} + \{F_{Gt}(t)\} \quad (3)$$

In Eq. (3) {F<sub>T</sub>(t)} represents the externally applied torque, and {F<sub>Gt</sub>(t)} represents the gear mesh induced moment. Note that Eqs. (1) to (3) repeat for each stage. The gear mesh forces couple the force equations of each stage to each other as well as the torsional equations to the lateral equations (Choy 1989; Cornell 1981; David 1987, 1988). The coupling relationships between the torsional and the lateral vibrations and the dynamics of each individual gear/rotor are derived in the next section.

#### COUPLING IN GEAR MESHES

The torsional and lateral vibration of each individual rotor stage and the dynamic relationships between all the gear stages are coupled through the nonlinear interactions in the gear mesh. Gear mesh forces and moments are evaluated as functions of relative motion and rotation between two meshing gears and the corresponding gear mesh stiffnesses. These gear mesh stiffnesses vary in a repeating nonlinear pattern (August 1986; Cornell 1981; Savage 1986) with each tooth pass engagement period and can be represented by a high order polynomial (Cornell 1981; Boyd 1987). A sixth order polynomial compliance curve is used in this study to simulate the stiffness changes for

contacting gear pairs (zero stiffness is input for noncontacting pairs). The repeatability of such nonlinear mesh stiffnesses can also act as a source of steady state excitation to the gear system. With the coordinate system as shown in Fig. 1 and with the effects of gear tooth surface friction neglected, the following gear mesh coupling equations can be established by equating force and moment in terms of base circle radius  $R_c$  (Choy 1989). For the  $k^{\text{th}}$  stage gear of the system, summing force in the x direction results in

$$F_{G_{xk}} = \sum_{i=1, i \neq k}^n K_{tki} \left[ -R_{ci} \theta_{ci} - R_{ck} \theta_{ck} + (X_{ci} - X_{ck}) \cos \alpha_{ki} + (Y_{ci} - Y_{ck}) \sin \alpha_{ki} \right] \cos \alpha_{ki} \quad (4)$$

Summing force in the y direction results in

$$F_{G_{yk}} = \sum_{i=1, i \neq k}^n K_{tki} \left[ -R_{ci} \theta_{ci} - R_{ck} \theta_{ck} + (X_{ci} - X_{ck}) \cos \alpha_{ki} + (Y_{ci} - Y_{ck}) \sin \alpha_{ki} \right] \sin \alpha_{ki} \quad (5)$$

Summing moment in the z direction results in

$$F_{G_{zk}} = \sum_{i=1, i \neq k}^n R_{ck} K_{tki} \left[ (-R_{ci} \theta_{ci} - R_{ck} \theta_{ck}) + (X_{ci} - X_{ck}) \cos \alpha_{ki} + (Y_{ci} - Y_{ck}) \sin \alpha_{ki} \right] \quad (6)$$

where  $n$  is the number of stages in the system. Damping forces in a similar form involving the relative velocities between the two mating gear stages would also be included.

#### MODAL ANALYSIS

To reduce the computational effort, the number of degrees-of-freedom of the system is reduced through modal transformation. Orthonormal modes for each individual rotor-bearing stage are obtained by solving the uncoupled

system homogeneous characteristic equations. Using the modal expansion approach (Choy 1987, 1988a, 1989), the motion of the system can be expressed as

$$\{X\} = \sum_{i=1}^m A_i \{\phi_i\} \quad (7)$$

$$\{Y\} = \sum_{i=1}^m B_i \{\phi_i\} \quad (8)$$

$$\{\theta\} = \sum_{i=1}^m A_{t_i} \{\phi_{t_i}\} \quad (9)$$

where  $m$  is the number of modes used to define each motion. The orthogonality conditions of the modes can be expressed as

$$\{\Phi\}^T [K] \{\Phi\} = \{\Lambda^2\} \quad (10)$$

where

$$K = \frac{K_{xx} + K_{yy}}{2 + K_s}$$

$$[\Phi_t]^T [K_T] [\Phi_t] = [\Lambda^2] \quad (11)$$

$$[\Phi]^T [M] [\Phi] = [\Phi_t]^T [J] [\Phi_t] = [I] \quad (12)$$

Using the modal expansion and the orthogonality conditions, with the bearing forces due the base motion expressed in the R.H.S., the modal equations of motion (Choy 1989) can be written:

For the X-Z equation

$$\begin{aligned} \{\ddot{A}\} + [\Phi]^T [G_v] [\Phi] \{\dot{B}\} + [\Phi]^T [C_{xx}] [\Phi] \{\dot{A}\} + [\Phi]^T [C_{xy}] [\Phi] \{\dot{B}\} + [\Phi]^T [G_A] [\Phi] \{B\} + [\Lambda^2] \{A\} \\ + [\Phi]^T [K_{dx}] [\Phi] \{A\} + [\Phi]^T [K_{xy}] [\Phi] \{B\} = [\Phi]^T \{F_x(t) + F_{gx}(t) + F_{Bx}(t)\} \end{aligned} \quad (13)$$

where

$$F_{Bx}(t) = [C_{xx}] \{\dot{X}_b\} + [C_{xy}] \{\dot{Y}_b\} + [K_{xx}] \{X_b\} + [K_{xy}] \{Y_b\} [K_{dx}] = [K_{xx}] - [K]$$

For the Y-Z equation

$$\begin{aligned} \{\ddot{B}\} - [\Phi]^T [G_v] [\Phi] \{\dot{A}\} + [\Phi]^T [C_{yx}] [\Phi] \{\dot{A}\} + [\Phi]^T [C_{yy}] [\Phi] \{\dot{B}\} - [\Phi]^T [G_A] [\Phi] \{A\} + [\Lambda^2] \{B\} \\ + [\Phi]^T [K_{dy}] [\Phi] \{B\} + [\Phi]^T [K_{yx}] [\Phi] \{A\} = [\Phi]^T \{F_y(t) + F_{gy}(t) + F_{By}(t)\} \end{aligned} \quad (14)$$

where

$$F_{By}(t) = [C_{xy}]\{\dot{X}_b\} + [C_{yy}]\{\dot{Y}_b\} + [K_{yx}]\{X_b\} + [K_{yy}]\{Y_b\} [K_{dy}] = [K_{yy}] - [K]$$

And for the  $\theta$ -equation

$$\{\ddot{A}_t\} + [\Phi_T]^T [C_T] [\Phi_t] \{\dot{A}_t\} + [\Lambda_t^2] \{A_t\} = [\Phi_t] \mathbb{I} \{F_t(t) + F_{Gt}(t)\} \quad (15)$$

The gear mesh forces and moments can also be expressed in the modal form, for the  $k^{\text{th}}$  stage with gear location at the  $l^{\text{th}}$  node, as

$$[\Phi]_k^T \{F_{Gx}\} = \sum_{j=1}^m \phi_{kjl} \left\{ \sum_{i=1, i \neq k}^n K_{tki} [-R_{ci} \theta_{ci} - R_{ck} \theta_{ck} + (X_{ci} - X_{ck}) \cos \alpha_{ki} + (Y_{ci} - Y_{ck}) \sin \alpha_{ki}] \cos \alpha_{ki} \right\} \quad (16)$$

$$[\Phi]_k^T \{F_{Gy}\} = \sum_{j=1}^m \phi_{kjl} \left\{ \sum_{i=1, i \neq k}^n K_{tki} [-R_{ci} \theta_{ci} - R_{ck} \theta_{ck} + (X_{ci} - X_{ck}) \cos \alpha_{ki} + (Y_{ci} - Y_{ck}) \sin \alpha_{ki}] \sin \alpha_{ki} \right\} \quad (17)$$

$$[\Phi]_k^T \{F_{Gt}\} = \sum_{j=1}^m \phi_{kjl} \left\{ \sum_{i=1, i \neq k}^n R_{ck} K_{tki} [(-R_{ci} \theta_{ci} - R_{ck} \theta_{ck}) + (X_{ci} - X_{ck}) \cos \alpha_{ki} + (Y_{ci} - Y_{ck}) \sin \alpha_{ki}] \right\} \quad (18)$$

where  $k$  is the stage number,  $j$  is the mode number, and  $l$  is the station location of the gear mesh.

#### SOLUTION PROCEDURE

Rearrange the modal equations of motion developed in Eqs. (13) to (15) into the following forms:

X-equation

$$\begin{aligned} \{\ddot{A}\} = & -[\Phi]^T[G_v][\Phi]\{\dot{B}\} - [\Phi]^T[C_{xx}][\Phi]\{\dot{A}\} - [\Phi]^T[C_{xy}][\Phi]\{\dot{B}\} - [\Phi]^T[G_A][\Phi]\{B\} - [\Lambda^2]\{A\} \\ & - [\Phi]^T[K_{dx}][\Phi]\{A\} - [\Phi]^T[K_{xy}][\Phi]\{B\} + [\Phi]^T\{F_x(t) + F_{Gx}(t) + F_{Bx}(t)\} \end{aligned} \quad (19)$$

Y-equation

$$\begin{aligned} \{\ddot{B}\} = & [\Phi]^T[G_v][\Phi]\{\dot{A}\} - [\Phi]^T[C_{yx}][\Phi]\{\dot{A}\} - [\Phi]^T[C_{yy}][\Phi]\{\dot{B}\} + [\Phi]^T[G_A][\Phi]\{A\} - [\Lambda^2]\{B\} \\ & \times [\Phi]^T + [K_{dy}][\Phi]\{B\} - [\Phi]^T[K_{yx}][\Phi]\{A\} + [\Phi]^T\{F_y(t) + F_{Gy}(t) + F_{By}(t)\} \end{aligned} \quad (20)$$

$\theta$ -equation

$$\{\ddot{A}_t\} = -[\Phi_t]^T[C_T][\Phi_t]\{\dot{A}_t\} - [\Lambda_t^2]\{A_t\} + [\Phi_t]^T\{F_t(t) + F_{Gt}(t)\} \quad (21)$$

A variable time stepping Newmark-Beta integration scheme evaluates the modal velocity and displacement at each time interval for each stage. In turn, Eqs. (7) to (9) transform the modal displacements into absolute displacements in fixed coordinates. The gear mesh forces can be evaluated by the relative

motion between the gear teeth using the nonlinear stiffnesses developed for the gear mesh interaction. The effects of gear box vibration can be calculated as nonlinear bearing forces through the relative vibration between the gear box and the shaft at the bearing locations. Since the gear box and the shaft are vibrating independently, a separate transient integration scheme is required for each system at every time step before the coupling of bearing forces.

#### DISCUSSION OF RESULTS

To demonstrate the application of the discussed analytical method, a typical three-stage gear transmission, given in Fig. 2, is used as an example. All three gear stages have an identical 36 tooth gear and a mesh contact ratio of 1.6. Stage I of the system is the driver with a rotational speed of 1500 rpm and an input torque of 2.25 kN·m. Both stages I and II are supported by three bearings; stage III only has two bearing supports. The first two bearings in stages I to III and the third bearing in stages I and II are identical. The rotors in stages I and II are of 2.4 in. in diameter and are of length of 40 and 30 in., respectively. The rotor in stage III is smaller with a diameter of 1.4 in. and a length of 20 in. For demonstration purposes, the first three basic lateral and two torsional modes of the system are used in the modal analysis (numerical experiment shows that the first three basic lateral modes accounts for over 90 percent of the system vibrations). Table I provides the information on the modal frequencies of the system in both lateral and torsional directions. Figures 3 and 4 give the orthonormal mode shapes of the first two basic torsional and lateral modes for all three rotor stages. (Third lateral mode shape and its modal excitations are omitted from the figures because of the mode shape's small magnitude in vibration).

In order to investigate the effects of gear box vibrations and rotor mass-imbalance, results from four major cases of external excitations are examined in this study:

Case 1: no gear box vibration and small mass-imbalance

Case 2: gear box vibration in x-direction and small mass-imbalance

Case 3: no gear box vibration and large mass-imbalance

Case 4: gear box vibration in x-direction and large mass-imbalance

The gear box vibrational effects are assumed to be a steady state vibratory motion of 600 Hz in the x direction at the bearing supports and to be unaffected by shaft vibrations. In addition to the damping characteristics due to the bearing supports, a 1-percent modal damping is assumed at the gear mesh. An initial condition of 0 velocity and displacement is used in this study. Vibrational orbits of all three rotor stages at the gear location for all four cases are given in Figs. 5 to 7. Note that the vibratory characteristics of stage I are more influenced by mass-imbalance while those of stages II and III are more affected by motion of the gear box through the bearing supports. As we can see from case 2 of Fig. 5(b), the effects of bearing support motion on stage I gear vibrational orbits are quite small. This is due to the fact that the rotor of stage I is substantially more flexible than the other two rotors and less influence from the bearing can be effectively converted to the system. In addition, although similar mass-imbalance are applied to each rotor stage, vibratory orbits in stages II and III are smaller in amplitude because of their larger rotor stiffnesses.

Figures 8 to 10 depict the x direction first modal component for rotor stages I to III, respectively. Figure 8 shows the effects of the four external excitations on the first modal vibratory component of stage I in both

time and frequency domains. Note that Fig. 8(a) shows that, for small imbalance with no gear box motion, only very small vibratory motion will result, except for the dc component at 0 frequency (due to the x direction displacement of the center of the orbit from the original journal position). Figures 8(b) represent the first mode rotor vibrations resulting from gear box motion. Note that the major component occurs at 600 Hz (input vibratory frequency at the bearing supports) with a minor component at 115 Hz (first natural frequency of stage I). Figures 8(c) show the effect of mass-imbalance which results in a large component at the rotor speed of 25 Hz and a smaller component at the first mode of 115 Hz. Figures 8(d) produce the combined effect of gear-box vibration and imbalance on rotor first mode vibrations. By examining the relative amplitudes of the two major components, at rotor speed and input frequency, with their corresponding input excitation magnitude, the sensitivity of the rotor to imbalance and gear-box vibration can be determined. Similar conclusions can be arrived in Figs. 9 and 10 for stages II and III except that the effects of mass-imbalance on first mode vibration is significantly reduced. As we can see in Figs. 9(d) and 10(d), when both excitations are presented, the gear-box motion has a much more dominating effect in rotor vibrations for stages II and III then for stage I.

Figures 11 to 13 show the vibration of the second mode component for the three rotor stages. Note that for stage I, the second mode vibrational characteristics are very similar to those of the first mode (Fig. 11). However, actual magnitudes are approximately 20 percent lower than those of the first mode. This is due to the fact that the first mode is more easily excited by the imbalance as well as by the bearing support excitations. Similar trends of vibrational effects can also be seen in the rotor motions in

stages II and III (Figs. 12 and 13). Note that the second modal frequency is not excited in this case, which further confirms the high excitability of the first mode. In addition, none of the torsional vibratory frequencies and gear meshing frequencies are excited in the lateral rotor vibration of the system (Figs. 8 to 13).

Figure 14 depicts the gear mesh forces with effects of both imbalance and gear-box motion excitations. Note that the major component of these forces are the dc component at 0 frequency due to the constant applying torque. The other sizable force component is at the tooth meshing frequency of 900 Hz. The higher ac component from the meshing of gears I and III results from the lower rotational stiffness in the stage III rotor. The effect of this lower rotational stiffness is also shown by the higher dc (0 frequency) component in stage III compared with stage II (Figs. 15 and 16). Only very small trace of force components can be observed at the gear mesh frequency (900 Hz) and first mode torsional frequencies of stage I (355 Hz), stage II (550 Hz), and stage III (280 Hz). Again, Figs. 15 and 16 outline the modal rotational vibration characteristics of all three rotor stages with both excitations. Note in Fig. 15 that other than the 0 frequency component, the other sizable vibration is at its own rotational modal frequency (i.e., 355 Hz at stage I, 550 Hz at stage II, and 280 Hz at stage III). Figure 16 depicts the second mode rotational vibration characteristics. Note that similar conclusions can be reached for the second modal frequencies of 1090, 1610, and 820 Hz, respectively, for stages I to III.

#### SUMMARY

This paper presents a vibration analysis with the effects of gear box motion and mass-imbalance for a multistage gear transmission. The analysis

combines gear mesh dynamics and structural modal analysis to study the transmission vibrations. The major content of this work can be summarized as follows:

1. A comprehensive approach is developed to combine the nonlinear gear mesh dynamics with structural lateral and torsional vibration of the system to determine the global system response.

2. The modal method transforms the equations of motion into modal coordinates to reduce the degree-of-freedom of the system.

3. Gear force observations in both the time and frequency domains provide good insights into the source of dominating response forces.

4. The magnitude of the gear mesh force is inversely proportional to the rotor stiffness of the driven system.

5. The influence of the gear box motion on system vibration is more pronounced in a stiffer rotor system.

6. Gear tooth mesh frequency and torsional modal frequencies have substantial effects on rotational but not on lateral vibrations of the system.

7. Knowledge of modal amplifications under various excitations provide an understanding of the vibrational characteristics of the system. This knowledge is crucial for designing transmissions with improved performance and durability.

#### REFERENCES

1. August, R., and Kasuba, R., 1986, "Torsional Vibrations and Dynamic Loads in a Basic Planetary Gear System," Journal of Vibration, Acoustics, Stress, and Reliability in Design, Vol. 108, No. 3, pp. 348-353.

2. Choy, F.K., and Li, W., 1987, "Frequency Component and Modal Synthesis Analysis of Large Rotor/Bearing Systems with Base Motion Induced Excitations," The Journal of Franklin Institute, Vol. 323, No. 2, pp. 145-168.
3. Choy, F.K., Padovan, J., and Li, W., 1988a, "Rub in High Performance Turbomachinery: Modeling; Solution Methodology; and Signature Analysis," Mechanical Systems and Signal Processing, Vol. 2, No. 2, pp. 113-133.
4. Choy, F.K., Townsend, D.P., and Oswald, F.B., 1988b, Dynamic Analysis of Multimesh-Gear Helicopter Transmissions, NASA TP-2789.
5. Choy, F.K., Tu, Y.K., Savage, M., and Townsend, D.P., 1989, "Vibration Signature Analysis of Multistage Gear Transmission," 1989 International Power Transmission and Gearing Conference, 5th Chicago, IL, Apr. 25-28, (1989), Proceedings, ASME, New York, Vol. 1, pp. 383-390. (Also NASA TM-101442.)
6. Cornell, R.W., 1981, "Compliance and Stress Sensitivity of Spur Gear Teeth," Journal of Mechanical Design, Vol. 103, No. 2, pp. 447-459.
7. David, J.W., and Park, N., 1987, "The Vibration Problem In Gear Coupled Rotor Systems," Advanced Topics in Vibrations; Proceedings of the Eleventh Biennial Conference on Mechanical Vibration and Noise, Boston, MA; Sept, 27-30, 1987, T.C. Huang and A.V. Karvelis, eds., ASME, New York, Vol. 1, pp. 297-304.
8. David, J.W., Mitchell, L.D., and Daws, J.W., 1988, "Using Transfer Matrices for Parametric System Forced Response," Journal of Vibration, Acoustics, Stress and Reliability in Design, Vol. 109, No. 4, pp. 356-360.

9. Lin, H., Huston, R.L., and Coy, J.J., 1988, "On Dynamic Loads in Parallel Shaft Transmissions: Part I - Modeling and Analysis," Journal of Mechanisms, Transmissions and Automation in Design, Vol. 110, No. 2, pp. 221 (Also, NASA TM-100180, 1987.)
10. Boyd, L.S., and Pike, J.A., 1987, "Epicyclic Gear Dynamics," AIAA Paper 87-2042, June.
11. Mitchell, L.D., and David, J.W., 1985, "Proposed Solution Methodology for the Dynamically Coupled Nonlinear Geared Rotor Mechanics Equations," Journal of Vibration, Acoustics, Stress, and Reliability in Design, Vol. 107, No. 1, pp. 112-116.
12. Savage, M., Caldwell, R.J., Wisor, J.W., and Lewicki, D.G., 1986, "Gear Mesh Compliance Modeling," Specialists' Meeting on Rotary Wing Propulsion Systems, Williamsburg, VA, Nov. 12-14, 1986; Technical Papers, American Helicopter Society, Alexandria, VA. (Also, NASA TM-88843, 1986.)

TABLE I. - SYSTEM NATURAL

FREQUENCIES

Mode	Stage 1	Stage 2	Stage 3
Torsion natural frequency			
1	355	550	280
2	1090	1610	820
Lateral natural frequency, Hz			
1	115	160	110
2	145	189	200
3	190	264	260

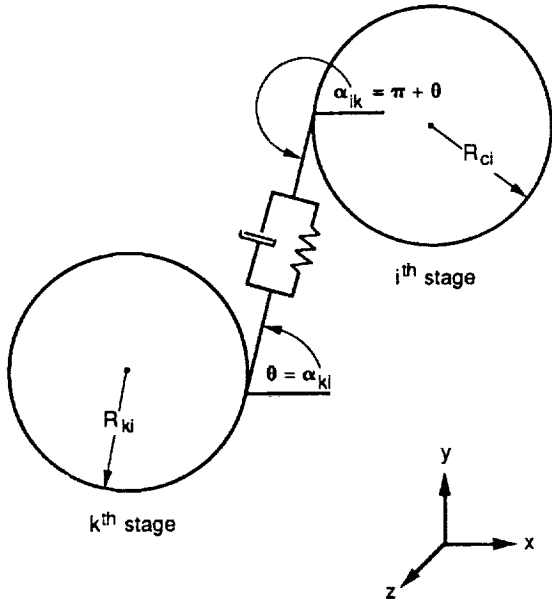


Figure 1.—Coordinate system for gear mesh force and moment.

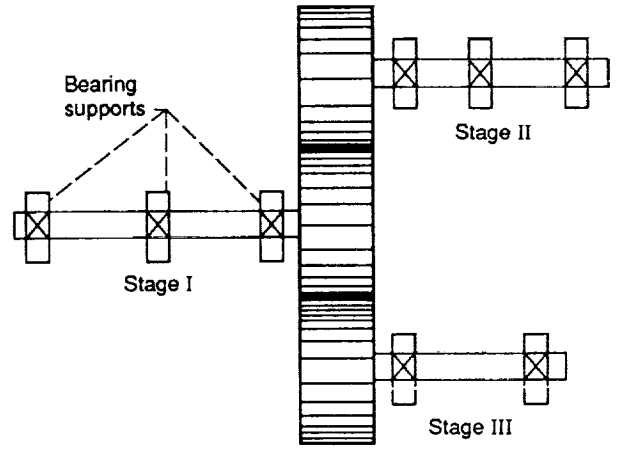


Figure 2.—Typical three stage rotor-bearing-gear system.

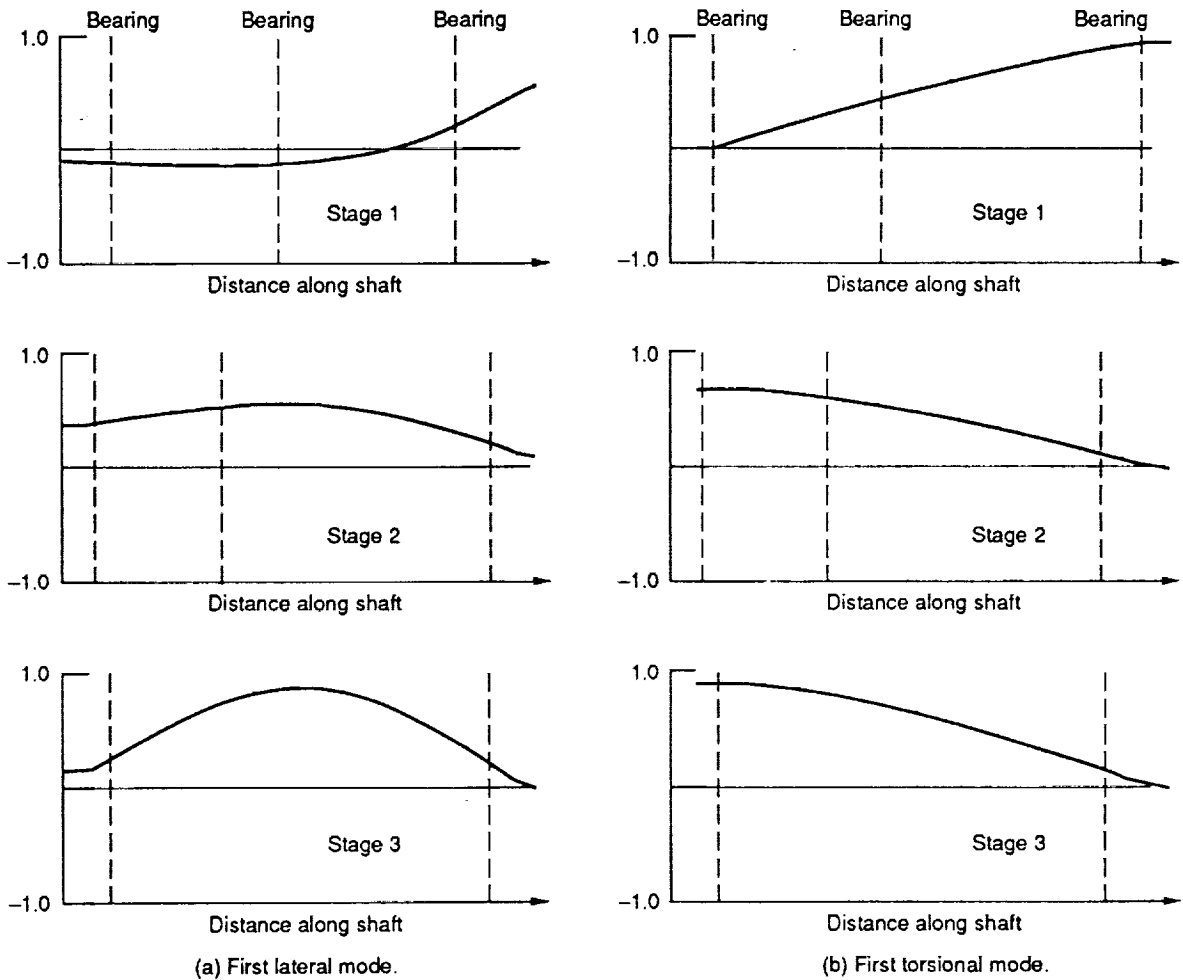


Figure 3.—First vibrational mode for the three-stage system.

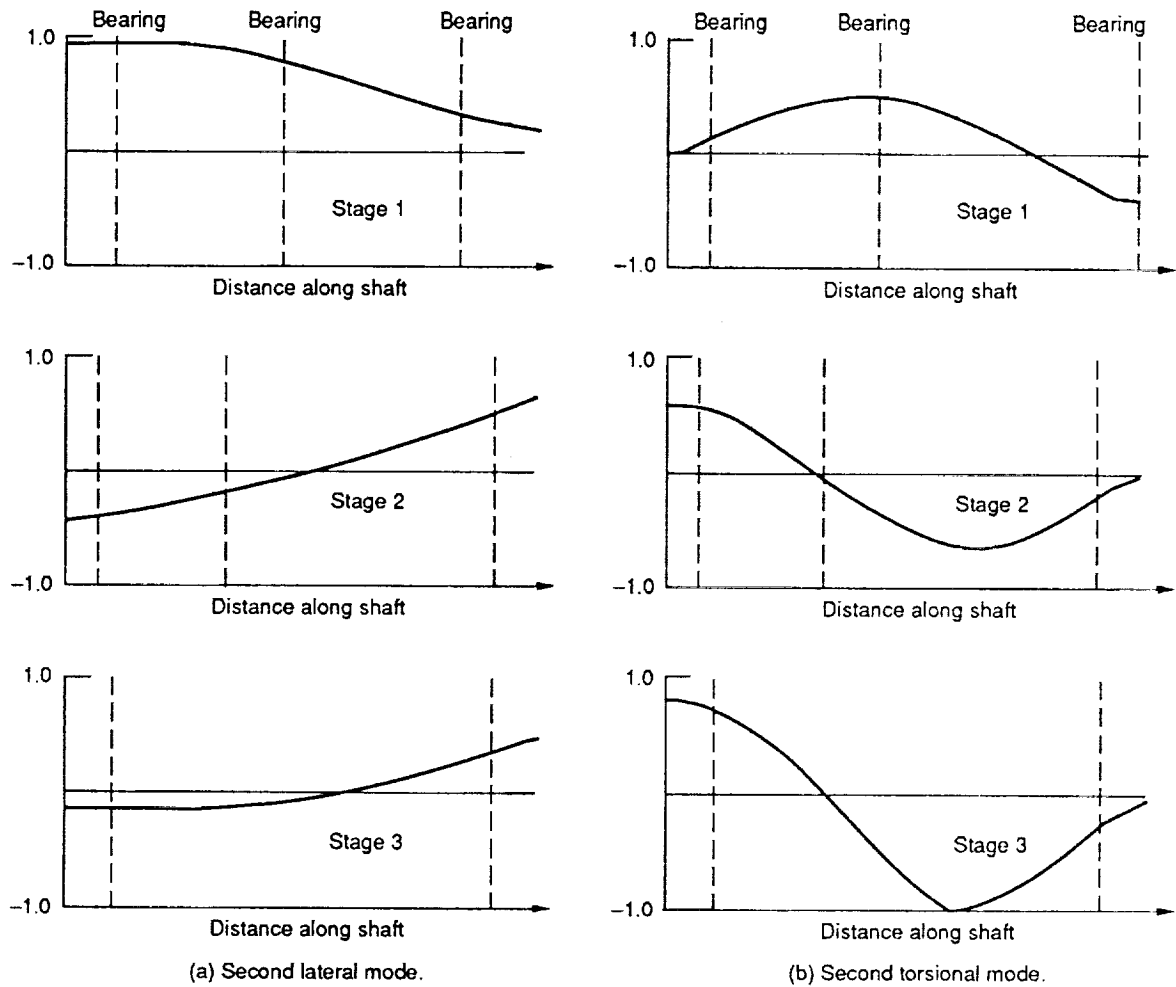


Figure 4.—Second vibrational mode for the three-stage system.

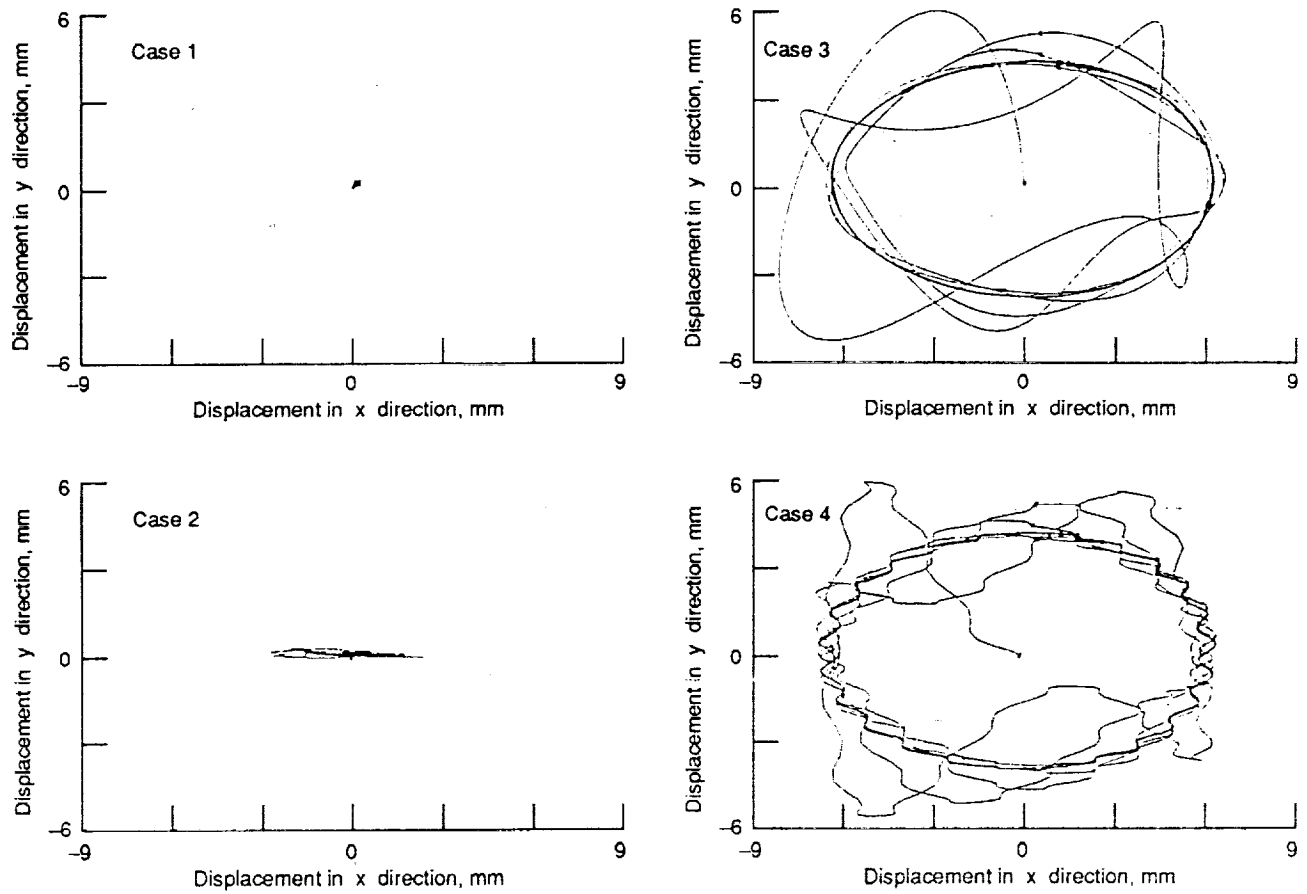


Figure 5.—Stage 1 rotor orbits under various load conditions.

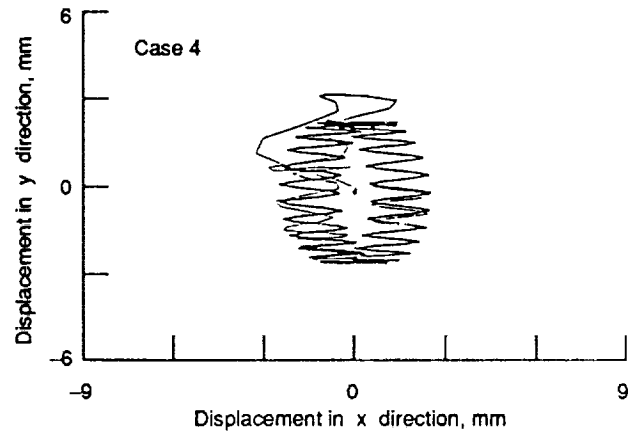
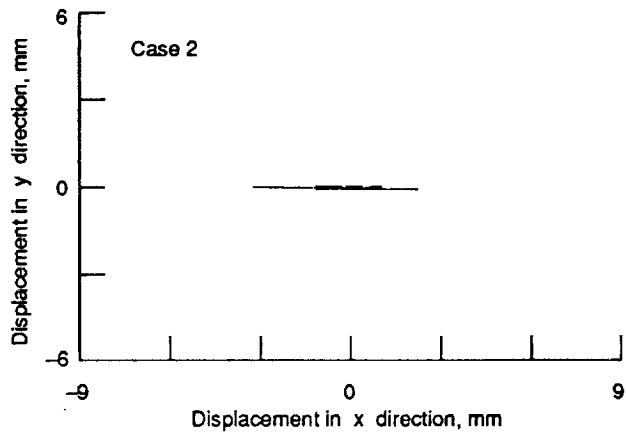
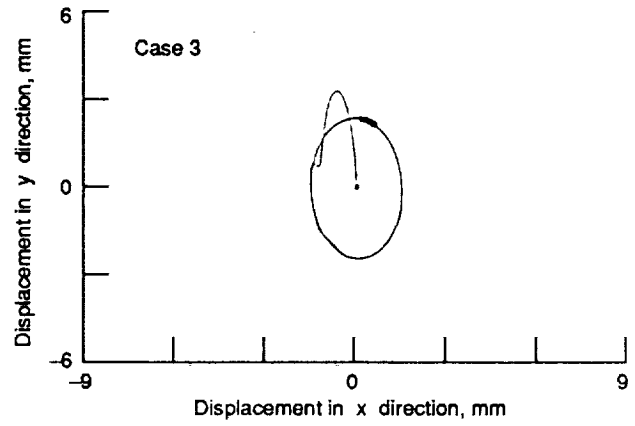
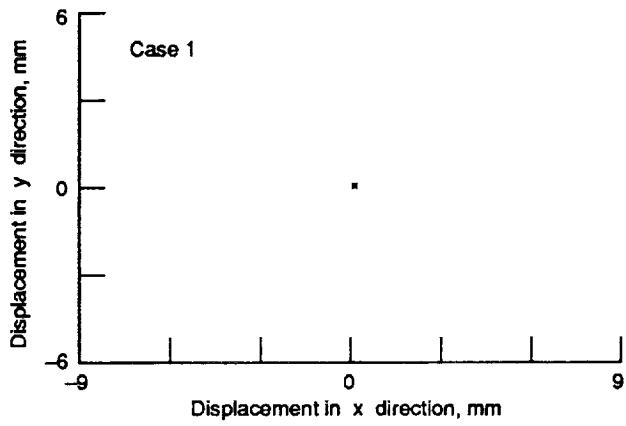


Figure 6.—Stage 2 rotor orbits under various load conditions.

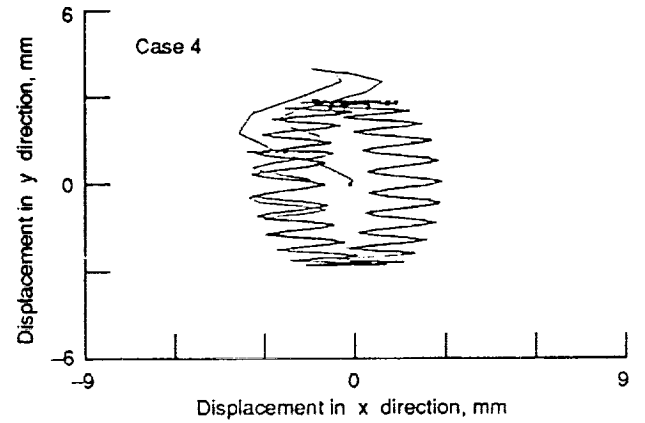
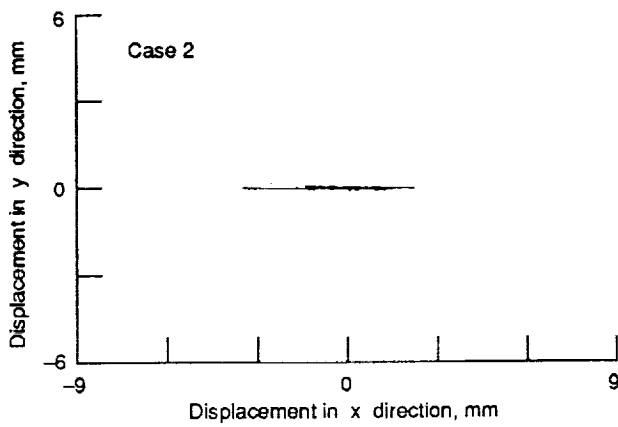
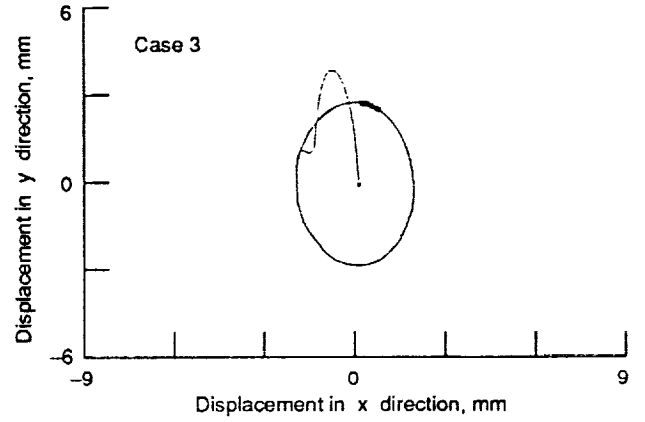
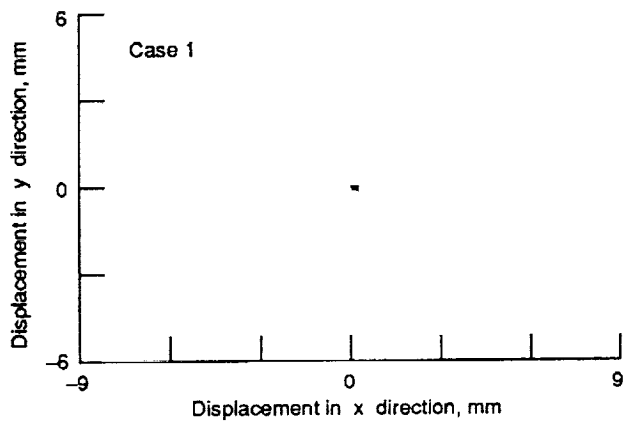
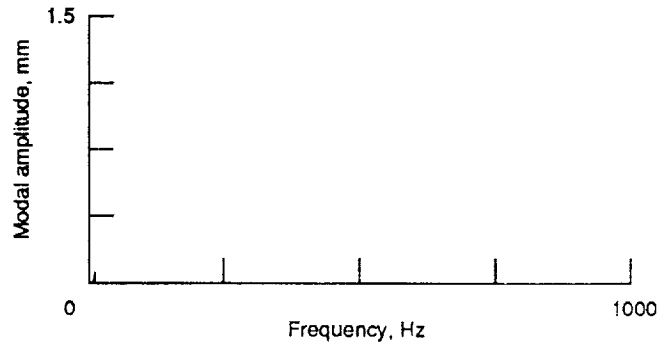
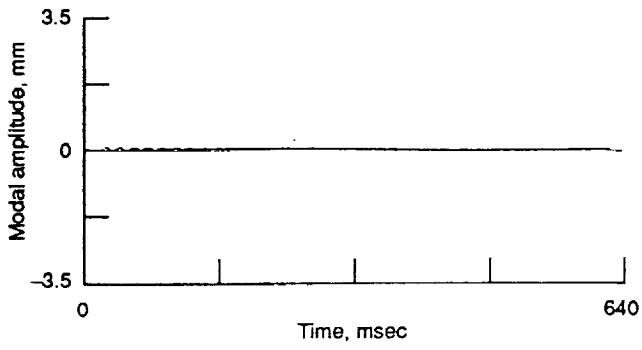
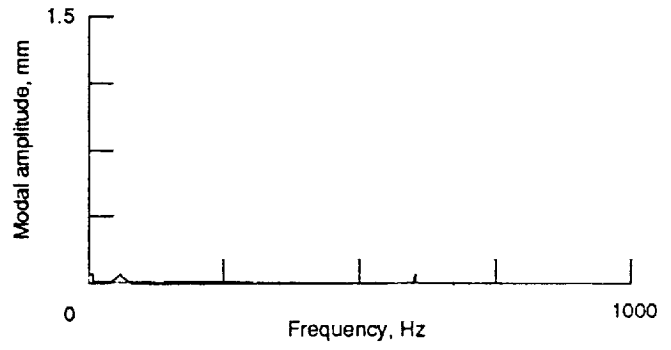
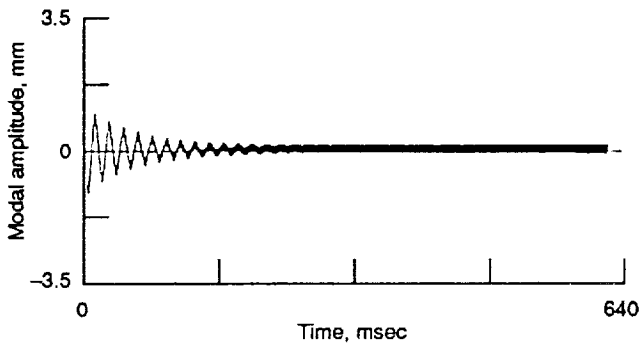


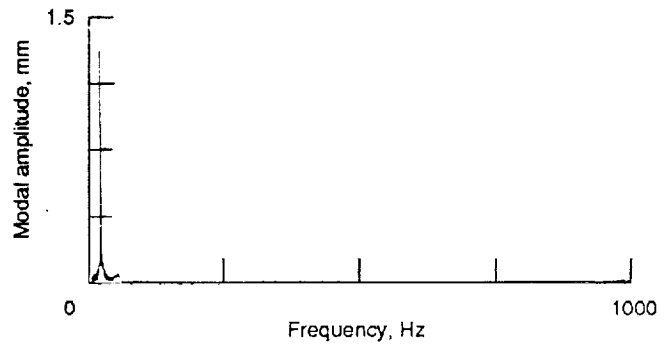
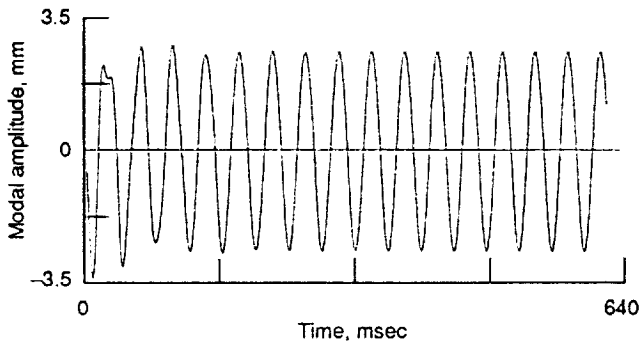
Figure 7.—Stage 3 rotor orbits under various load conditions.



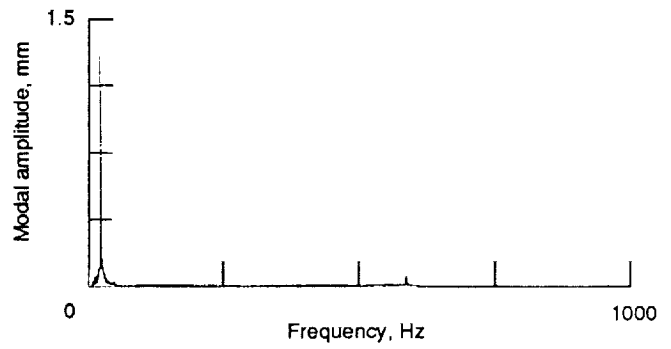
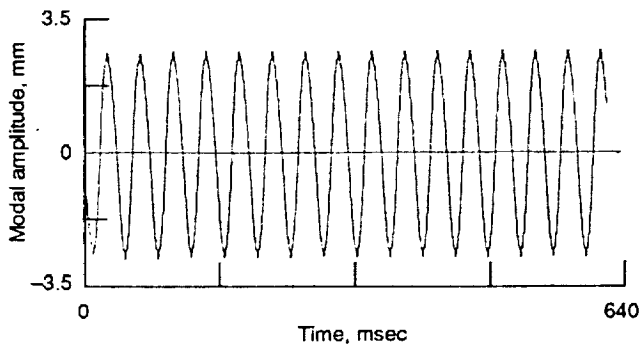
(a) Case 1.



(b) Case 2.

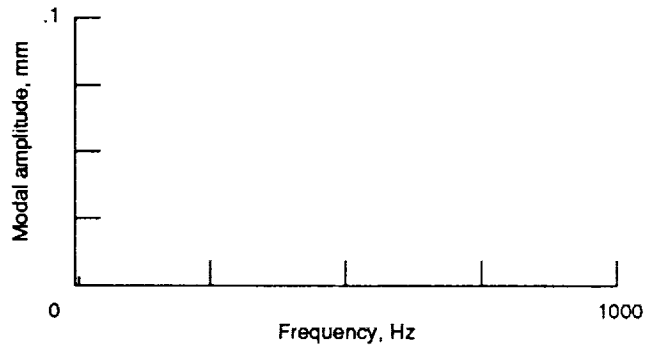
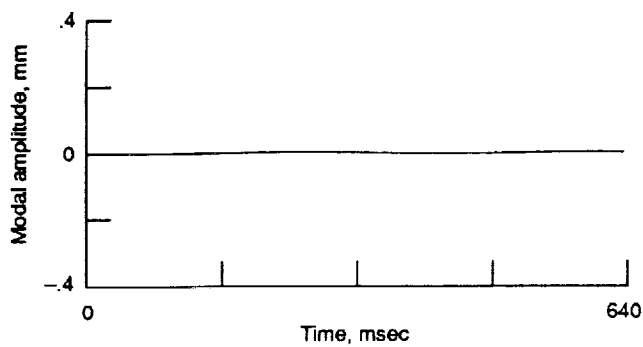


(c) Case 3.

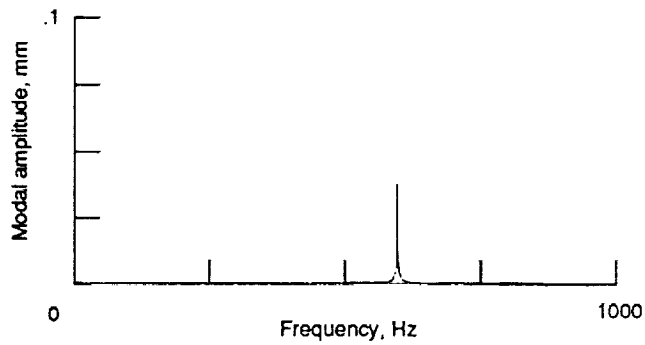
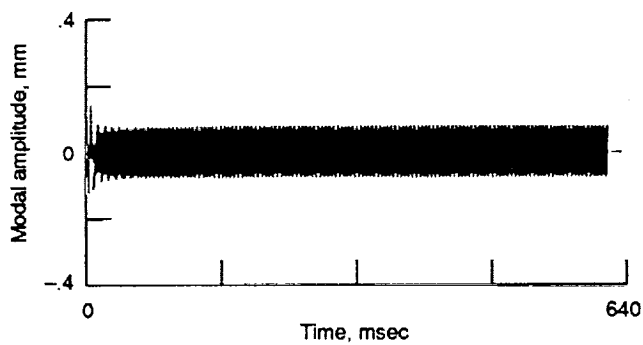


(d) Case 4.

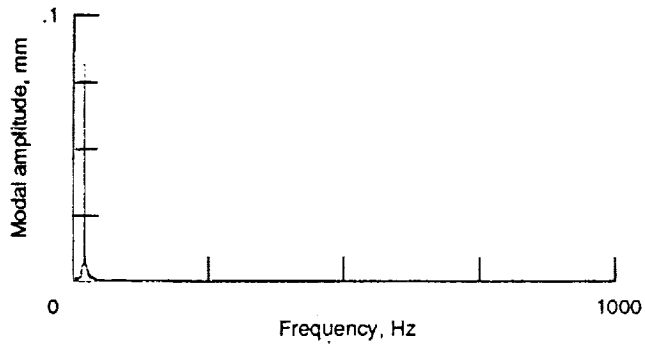
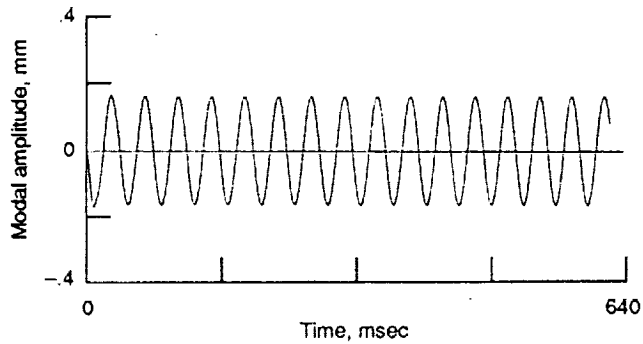
Figure 8.—Stage 1 modal excitations of the first lateral mode.



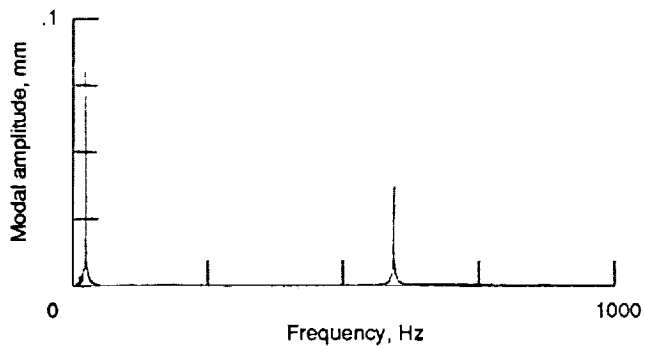
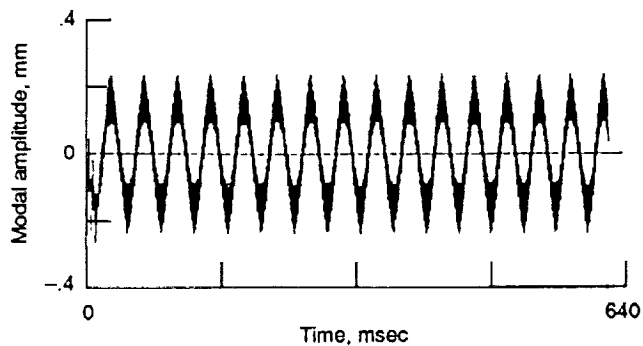
(a) Case 1.



(b) Case 2.

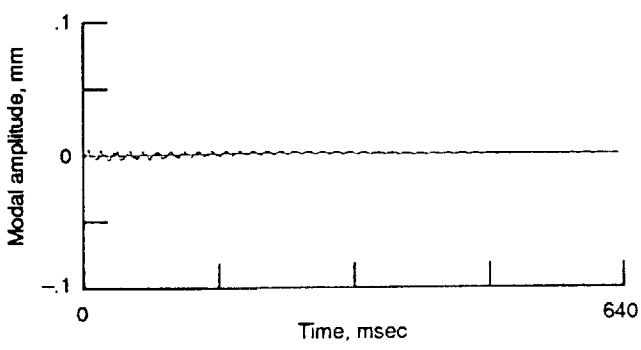


(c) Case 3.

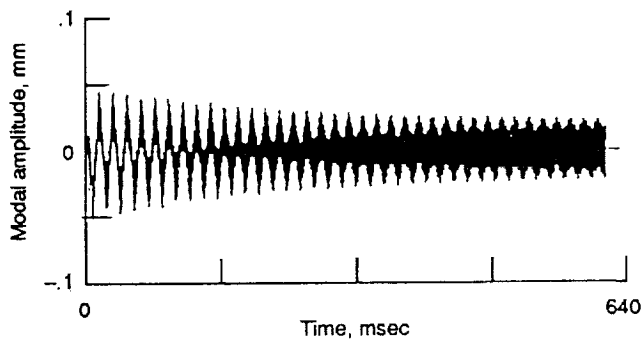
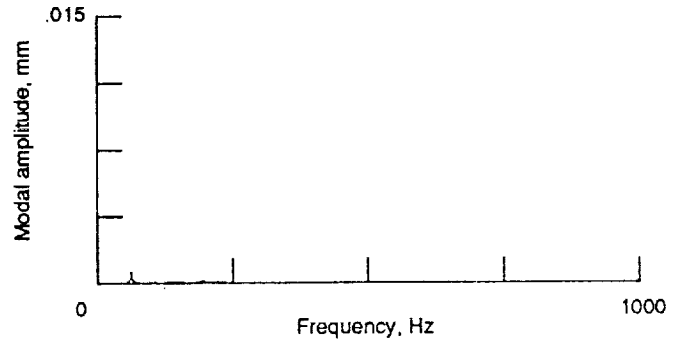


(d) Case 4.

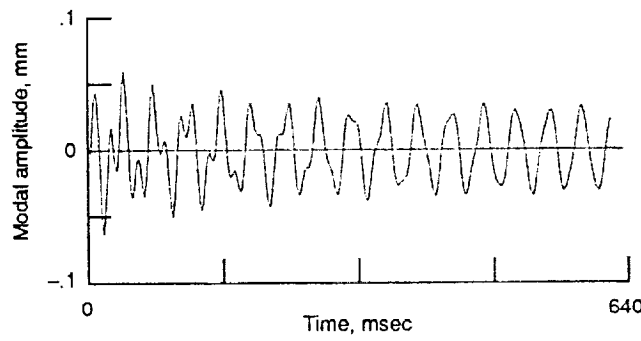
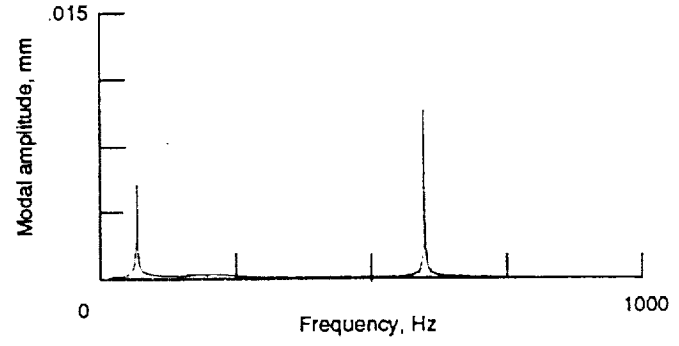
Figure 9.—Stage 2 modal excitations of the first lateral mode.



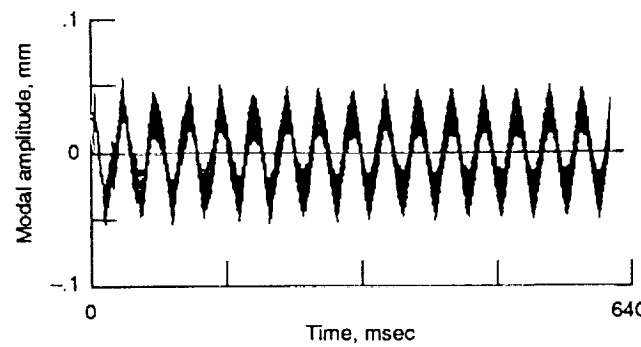
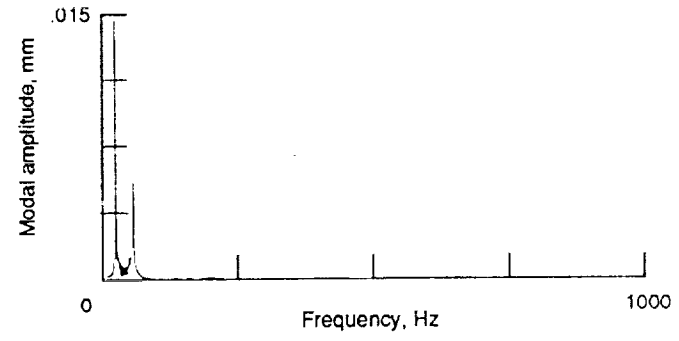
(a) Case 1.



(b) Case 2.



(c) Case 3.



(d) Case 4.

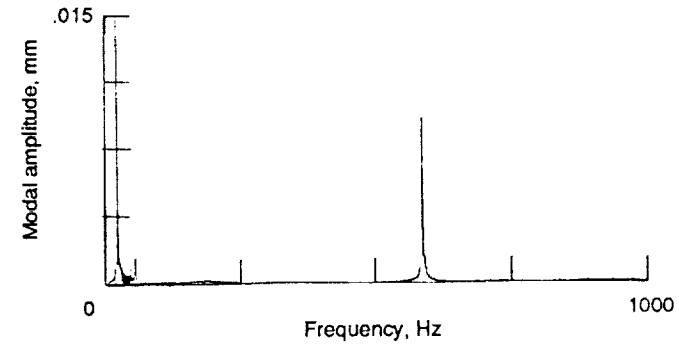
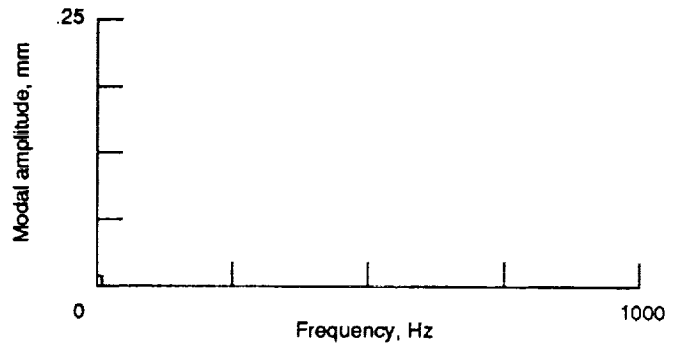
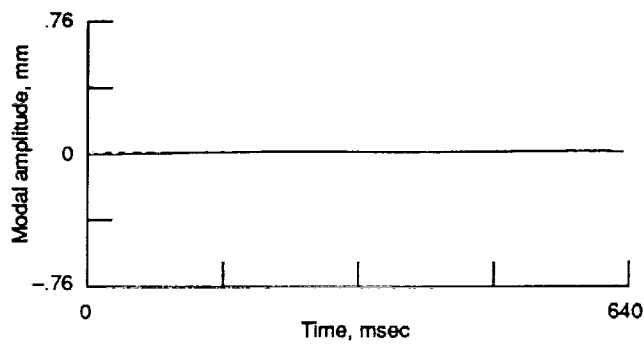
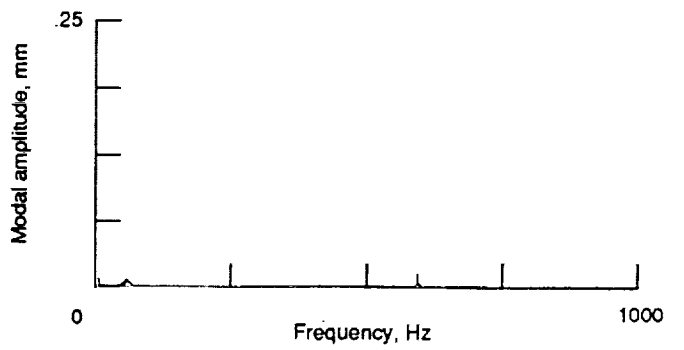
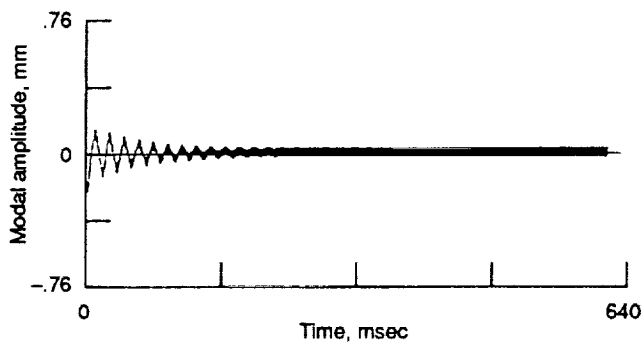


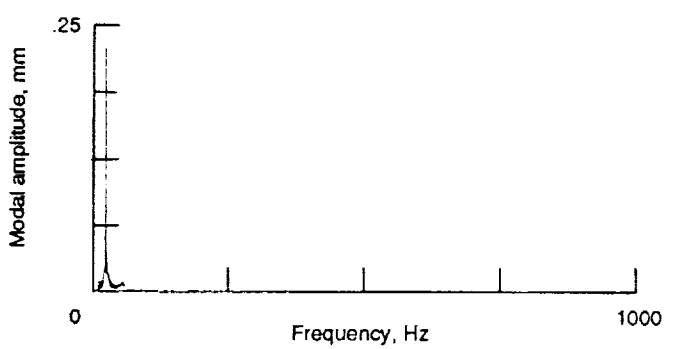
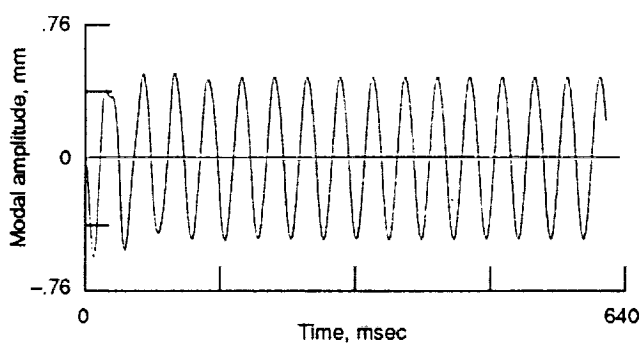
Figure 10.—Stage 3 modal excitations of the first lateral mode.



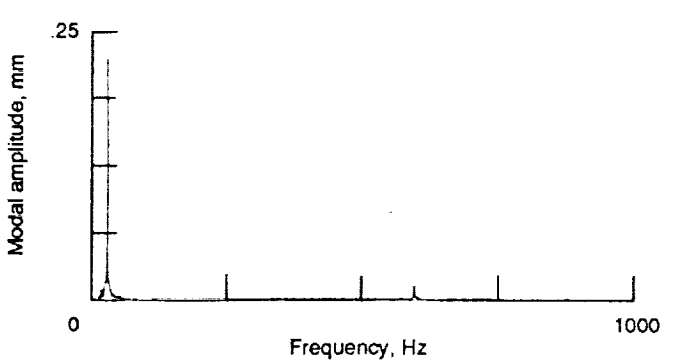
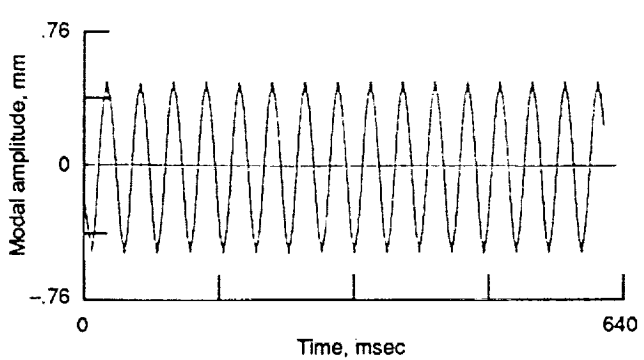
(a) Case 1.



(b) Case 2.

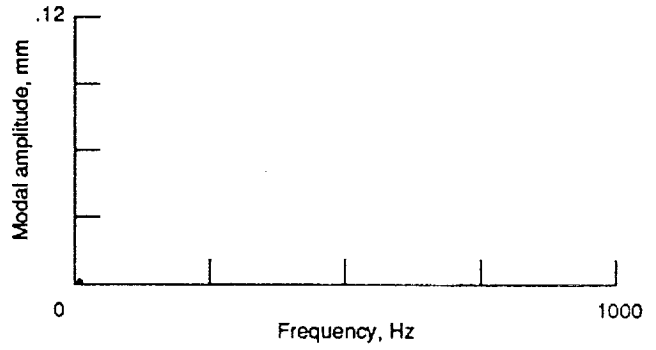
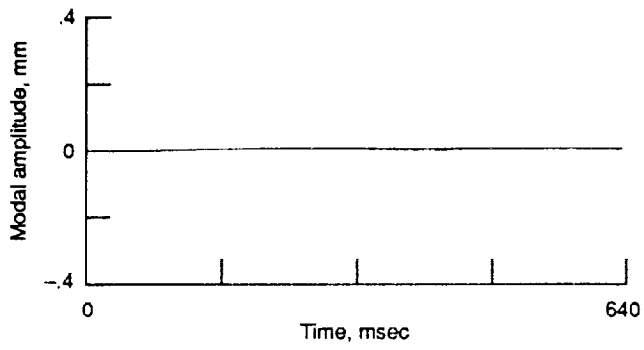


(c) Case 3.

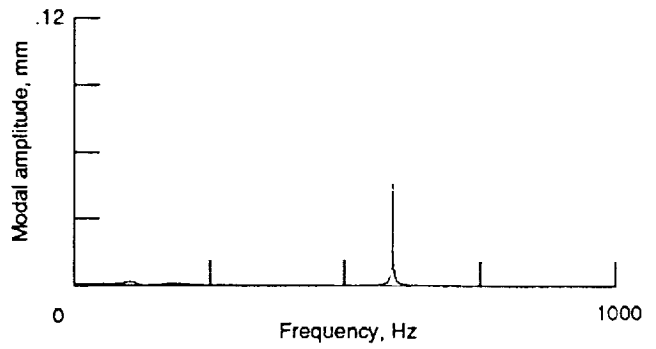
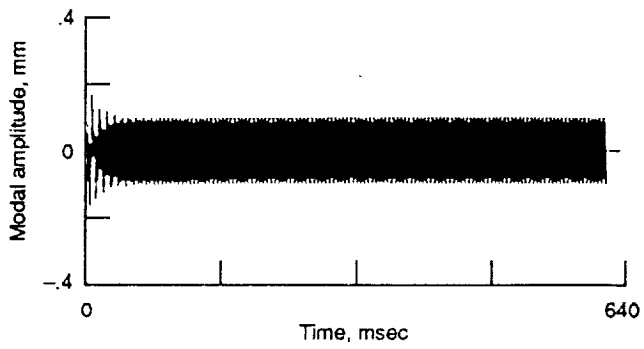


(d) Case 4.

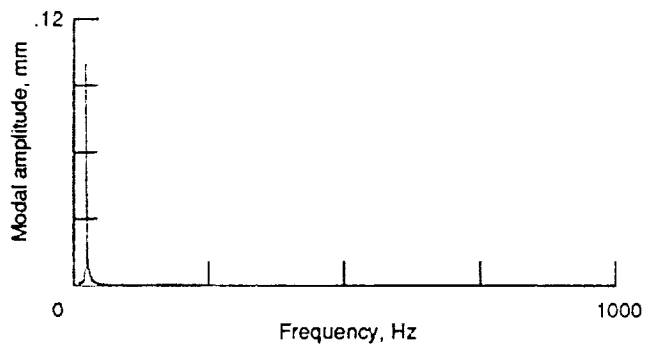
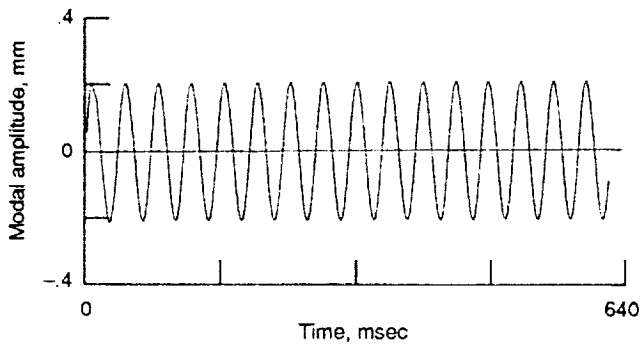
Figure 11.—Stage 1 modal excitations of the second lateral mode.



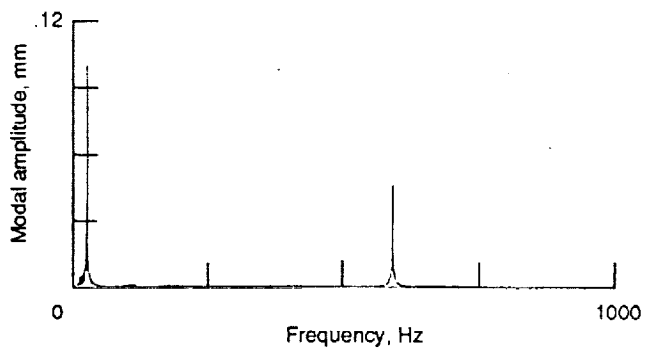
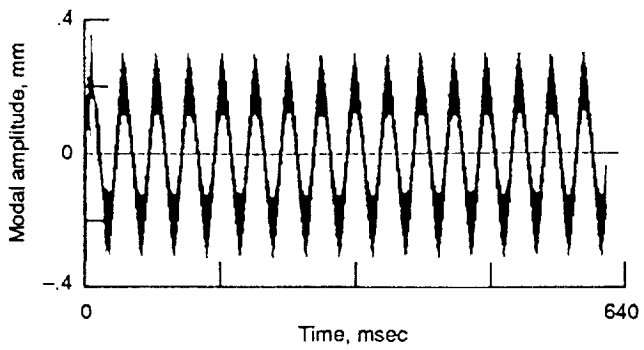
(a) Case 1.



(b) Case 2.

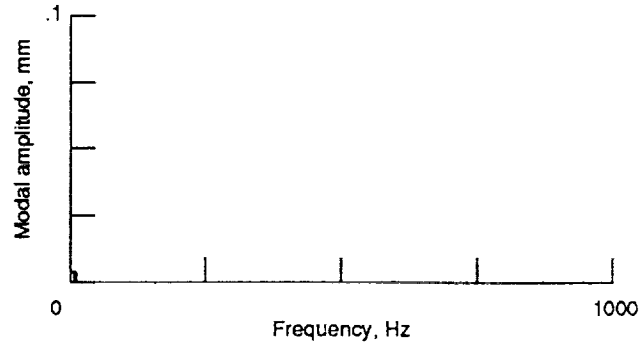
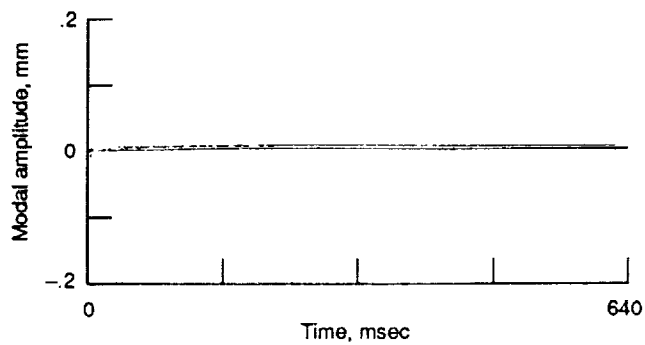


(c) Case 3.

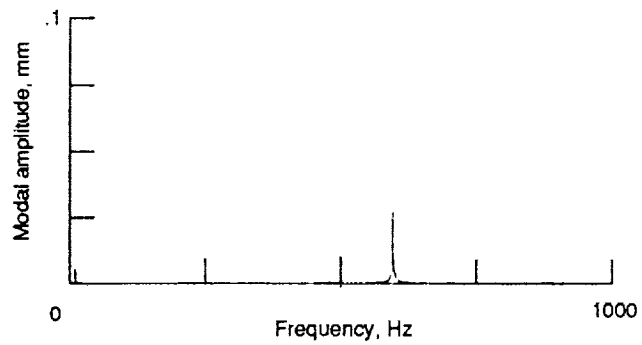
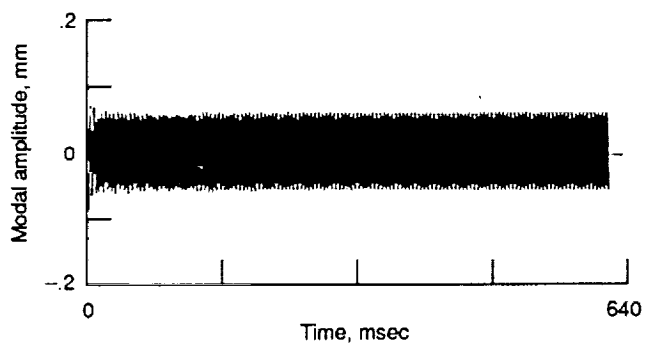


(d) Case 4.

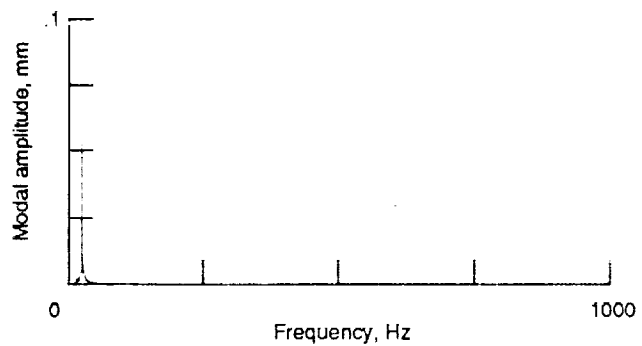
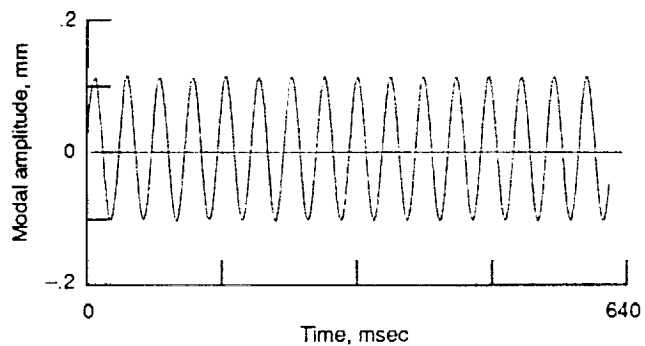
Figure 12.—Stage 2 modal excitations of the second lateral mode.



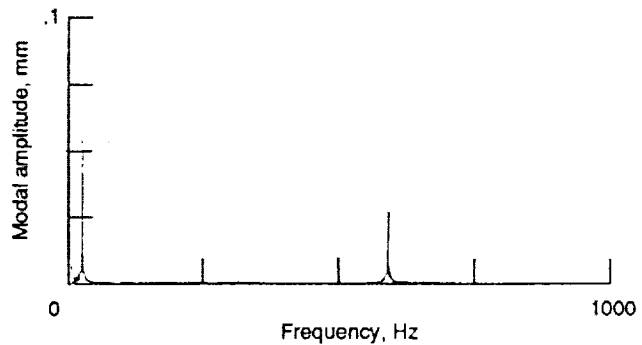
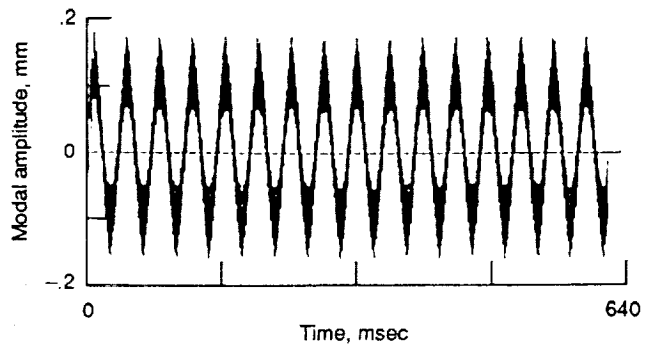
(a) Case 1.



(b) Case 2.

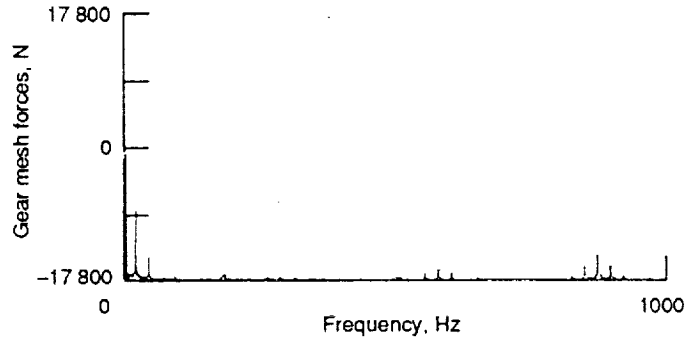
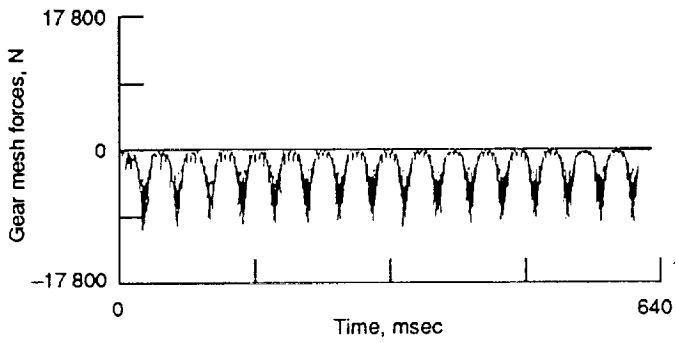


(c) Case 3.

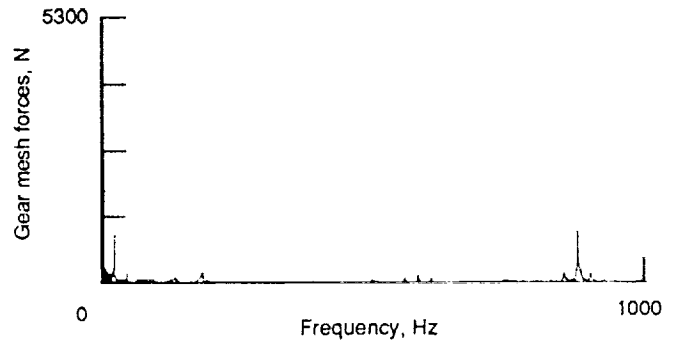
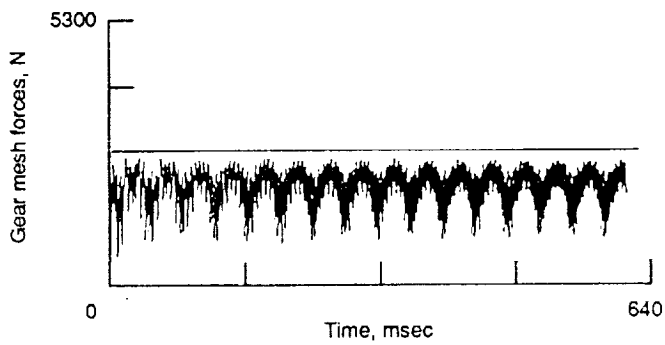


(d) Case 4.

Figure 13.—Stage 3 modal excitations of the second lateral mode.

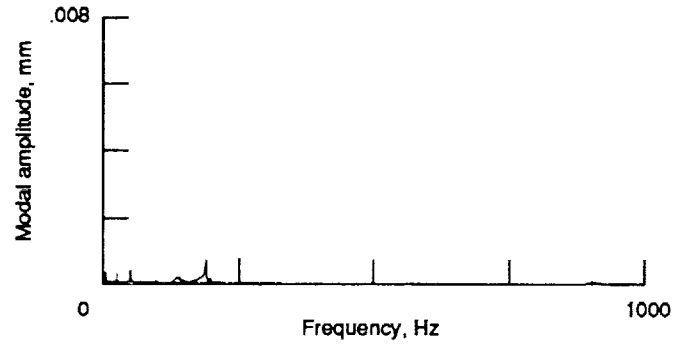
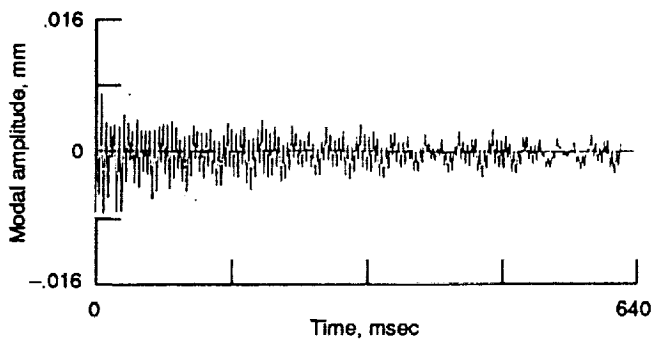


(a) Gear 1-2.

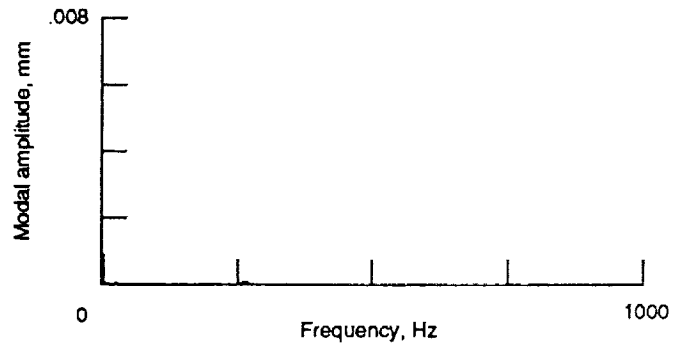
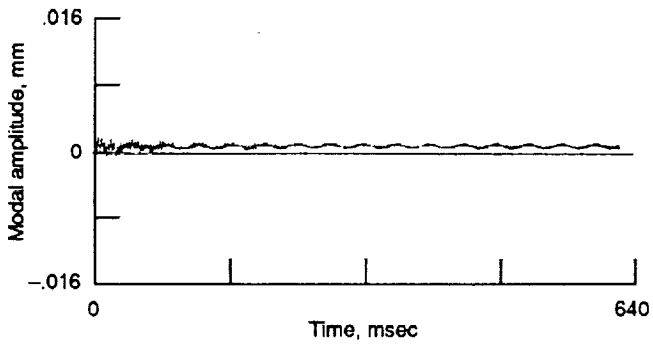


(b) Gear 1-3.

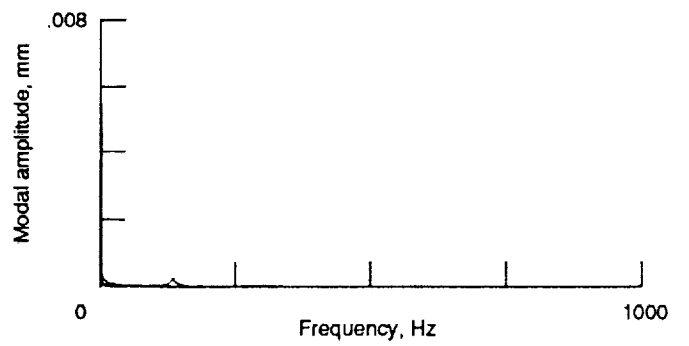
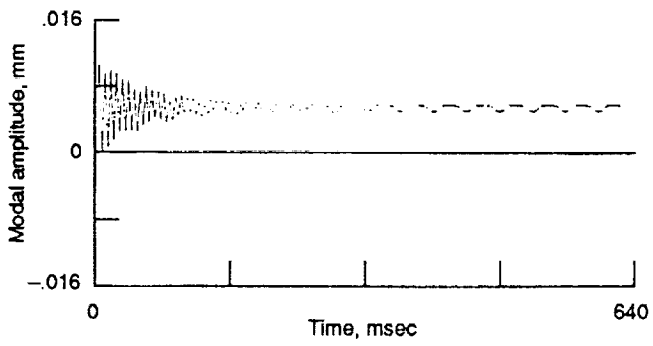
Figure 14.—Gear forces in time and frequency domains.



(a) Stage 1.

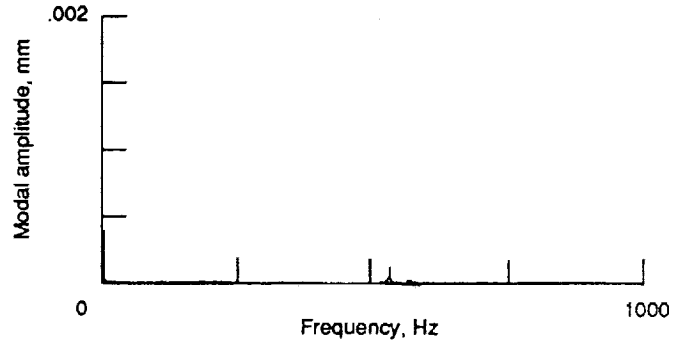
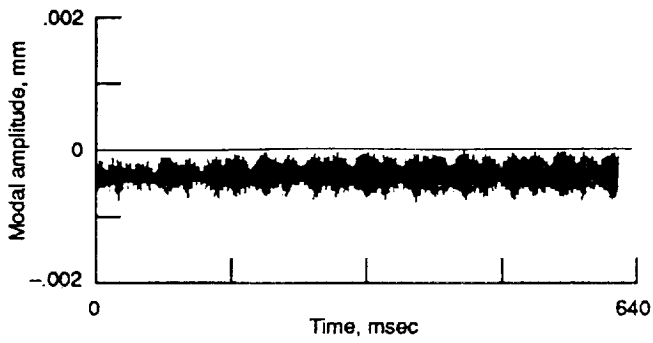


(b) Stage 2.

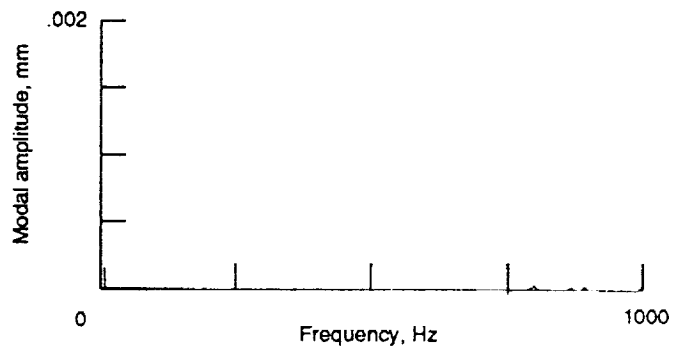
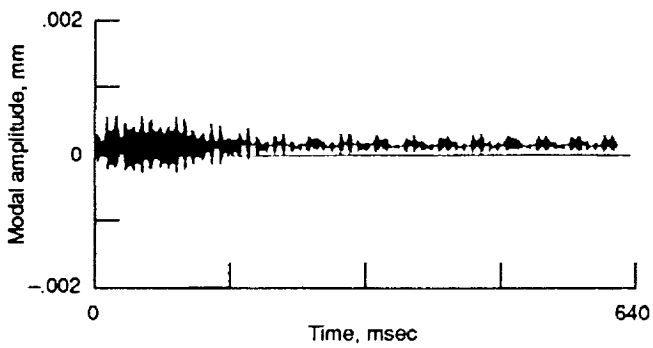


(c) Stage 3.

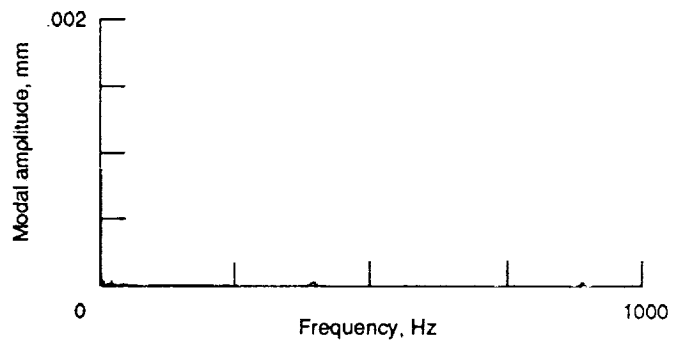
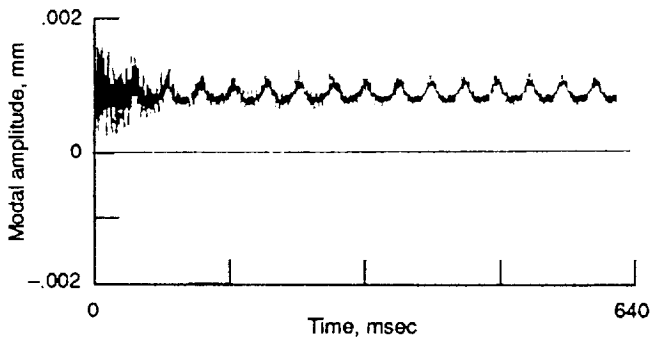
Figure 15.—Stage 1 modal excitations of the first torsional mode.



(a) Stage 1.



(b) Stage 2.



(c) Stage 3.

Figure 16.—State 1 modal excitations of the second torsional mode.

1. Report No. NASA TM-103695 AVSCOM TR 90-C-022		2. Government Accession No.		3. Recipient's Catalog No.	
4. Title and Subtitle Effects of Gear Box Vibration and Mass Imbalance on the Dynamics of Multi-Stage Gear Transmissions				5. Report Date March 1991	
				6. Performing Organization Code	
7. Author(s) Fred K. Choy, Yu K. Tu, James J. Zakrajsek, and Dennis P. Townsend				8. Performing Organization Report No. E-5916	
				10. Work Unit No. 505-63-51 1L162211A47A	
9. Performing Organization Name and Address NASA Lewis Research Center Cleveland, Ohio 44135-3191 and Propulsion Directorate U.S. Army Aviation Systems Command Cleveland, Ohio 44135-3191				11. Contract or Grant No.	
				13. Type of Report and Period Covered Technical Memorandum	
12. Sponsoring Agency Name and Address National Aeronautics and Space Administration Washington, D.C. 20546-0001 and U.S. Army Aviation Systems Command St. Louis, Mo. 63120-1798				14. Sponsoring Agency Code	
15. Supplementary Notes Fred K. Choy and Yu K. Tu, Department of Mechanical Engineering, The University of Akron, Akron, Ohio 44325; James J. Zakrajsek and Dennis P. Townsend, NASA Lewis Research Center.					
16. Abstract The objective of this paper is to present a comprehensive approach to analyzing the dynamic behavior of multistage gear transmission systems, with the effects of gear-box-induced vibrations and rotor mass-imbalance. The model method, using undamped frequencies and planar mode shapes, is used to reduce the degree-of-freedom of the system. The various rotor-bearing stages as well as the lateral and torsional vibrations of each individual stage are coupled through localized gear-mesh-tooth interactions. Gear-box vibrations are coupled to the gear stage dynamics through bearing support forces. Transient and steady state dynamics of lateral and torsional vibrations of the geared system are examined in both time and frequency domains. Vibration signature analysis techniques will be developed in interpret the overall systems dynamics and individual modal excitations under various operating conditions. A typical three-staged geared system is used as an example. Effects of mass-imbalance and gear box vibrations on the system dynamic behavior are presented in terms of modal excitation functions for both lateral and torsional vibrations. Operational characteristics and conclusions are drawn form the results presented.					
17. Key Words (Suggested by Author(s)) Gearbox; Vibrations; Dynamics; Multistage; Imbalance			18. Distribution Statement Unclassified - Unlimited Subject Category 37		
19. Security Classif. (of this report) Unclassified		20. Security Classif. (of this page) Unclassified		21. No. of pages 32	22. Price* A03